

1 **Synthesis, crystal structure and magnetic properties of a Cu(II) paddle-wheel complex with mixed**  
2 **bridges**

3  
4  
5 Joan Soldevila-Sanmartín <sup>a</sup>, José A. Ayllón <sup>a,\*</sup>, Teresa Calvet <sup>b</sup>, Merce Font-Bardia <sup>c</sup>, Concepción  
6 Domingo <sup>d</sup>, Josefina Pons <sup>a</sup>  
7  
8  
9  
10  
11  
12  
13  
14  
15  
16  
17

18 a Departament de Química, Universitat Autònoma de Barcelona, 08193, Bellaterra, Barcelona, Spain

19 b Cristal·lografia, Mineralogia i Dipòsits Minerals, Universitat de Barcelona, Martí i Franquès s/n, 08028 Barcelona, Spain

20 c Unitat de Difracció de Raig-X, Centres Científics i Tecnològics de la Universitat de Barcelona (CCiTUB), Universitat de  
21 Barcelona, Solé i Sabarís, 1-3, 08028 Barcelona, Spain

22 d Instituto de Ciencia de Materiales de Barcelona (CSIC), Campus UAB, 08193 Bellaterra, Spain  
23  
24  
25  
26  
27  
28  
29

30 \* Corresponding author.

31 E-mail address: [joseantonio.ayllon@uab.cat](mailto:joseantonio.ayllon@uab.cat) (J.A. Ayllón).  
32  
33

34 **ABSTRACT:**

35

36 The synthesis and characterization of a mixed carboxylate paddle-wheel copper complex, with formula  
37  $[\text{Cu}(\mu\text{-Pip})(\mu\text{-MeCO}_2)(\text{MeOH})]_2$  (Pip = piperonylate or 1,3-benzodioxole-5-carboxylate and MeCO<sub>2</sub> =  
38 acetate), is here reported. The described compound is a binuclear complex, each pair of similar  
39 carboxylate ligands occupying mutually trans bridging positions, while the methanol occupies the apical  
40 positions. The dimers are arranged into 2D layers in the bc plane through a network of O-H...O  
41 hydrogen bonds established between the methanol and the acetate ligand. Magnetic studies showed a  
42 strong antiferromagnetic Cu...Cu interaction ( $J = -308 \text{ cm}^{-1}$ ), in agreement with the presence of four  $\mu$ -  
43  $\kappa\text{O}-\kappa\text{O}'$  carboxylates bridging the metallic centers in the binuclear complex.

44

45

46

47

48

49

50

## 51 1. INTRODUCTION

52

53 Copper(II) complexes involving carboxylate ligands are particularly interesting due to the versatility of  
54 this ligand that can adopt different coordination modes, thus allowing the building of a wide range of  
55 structures [1–5]. The paddle-wheel structure is a very frequent architecture found for binuclear  
56 complexes. Until now, and only considering copper compounds, more than 1300 crystal structures that  
57 contain  $[\text{Cu}_2\text{L}_4]$  (L = carboxylate) core have been reported [6,7]. In these compounds, carboxylate  
58 ligands occupy the equatorial copper coordination positions, in a syn-syn coordination mode,  
59 establishing four bridges between the metal centers. Otherwise, the axial positions could be occupied by  
60 a variety of donor molecules. This structure is frequently found in different materials, from discrete  
61 complexes to 1D coordination polymers and in metal organic frameworks. In the vast majority of those  
62 compounds, all carboxylate ligands have the same nature, however, only eight mixed carboxylate  
63  $[\text{Cu}(\text{L})(\text{L}')(\text{X})_2]$  have been described [6,8–15], six of them having two acetate anion ligands [9–12, 14,  
64 15]. In a pair of these few examples, the presence of bulky carboxylate ligands could favor the  
65 formation of mixed carboxylates dimers [12,14].

66 We are interested in the synthesis of  $[\text{Cu}(\text{Pip})_2(\text{X})_2]$  (Pip = piperonylate, X = solvent) compounds, with  
67 the objective of replacing X for bulky amine derivatives, thus, aiming to build up novel supramolecular  
68 systems with potential applications in catalysis and gas storage/separation. During this investigation,  
69 crystals of  $[\text{Cu}(\mu\text{-Pip})(\mu\text{-MeCO}_2)(\text{MeOH})_2]$  were unexpectedly obtained while using MeOH as solvent  
70 and 1Cu:1Pip molar ratio, a new mixed carboxylate paddlewheel copper complex. Full characterization  
71 of this new compound is here presented, intending to understand the factors that favor the formation of  
72 mixed carboxylate paddle-wheel complexes. In the present case, there is not steric hindrance for the  
73 formation of homoleptic piperonylate, and in fact we have isolated a  $[\text{Cu}(\mu\text{-Pip})_2(\text{BzPy})_2]$  paddle wheel  
74 complex [16]. However, reported works discuss the effect of solvent's polarity in the formation of either  
75 the homoleptic or heteroleptic compounds [9]. A heteroleptic compound containing vanillinate and  
76 acetate ligands  $[\text{Cu}_2(\mu\text{-C}_8\text{H}_7\text{O}_4)(\mu\text{-MeCO}_2)(\text{MeOH})_2]$  is obtained when working in MeOH, whereas  
77 homoleptic compound  $[\text{Cu}_2(\text{C}_8\text{H}_7\text{O}_4)_4(\text{H}_2\text{O})_2]$  is obtained when working in H<sub>2</sub>O (C<sub>8</sub>H<sub>8</sub>O<sub>4</sub> = vanillic  
78 acid). In the present work, the designed synthetic method produces bulk quantities of  $[\text{Cu}(\mu\text{-Pip})(\mu\text{-}$   
79  $\text{MeCO}_2)(\text{MeOH})_2]$  complex, [17] whose structure is shown in Fig. 1. The obtained product is a green  
80 crystalline powder. The elemental analysis of this sample gives satisfactory C and H values. Moreover,  
81 powder X-ray diffraction shows that the structure of the bulk powder matches the one of the single-  
82 crystal, with only a small displacement of the peaks due to the different characterization temperature  
83 applied in the powder (room temperature) and monocrystal (100 K) measurements (Fig. 2).

84 ATR-FTIR spectrum of this compound shows significant shifts in the  $\nu(\text{C}=\text{O})$  and  $\nu(\text{C}\backslash\text{O})$  stretching  
85 with respect to the spectra of free ligands, hence confirming the coordination of the Cu(II) to the  
86 carboxylate groups of the Pip and MeCO<sub>2</sub> ligands. Additionally, the coordination mode of the  
87 carboxylate groups can be inferred from the difference between the asymmetry and symmetric

88 vibrations of the COO<sup>-</sup> groups ( $\Delta = \nu\text{COO}_{\text{asym}} - \nu\text{COO}_{\text{sym}}$ ) [18,19]. The values of the compound  
89 show a bidentate bridging mode for the carboxylate ligands [20–23]. Another characteristic band,  
90 appearing at 3279 cm<sup>-1</sup> and assignable to  $\nu(\text{O}\cdots\text{H})$  vibration, is in agreement with the presence of  
91 MeOH in the complex. The shape and position of this band suggest that the hydroxyl group participates  
92 in a hydrogen bond interaction [22,23].

93 The structure was determined by single crystal X-ray diffraction [24]. X-ray studies confirmed that the  
94 compound  $[\text{Cu}(\mu\text{-Pip})(\mu\text{-MeCO}_2)(\text{MeOH})]_2$  has a paddle-wheel binuclear Cu(II) structure, with four  
95 bridging carboxylate ligands in a syn-syn coordination mode (Fig. 1). Each Cu metal atom was  
96 coordinated to five oxygen atoms, four from different carboxylate groups (two of Pip ligands and two of  
97 acetate groups) at the equatorial positions and another oxygen atom from MeOH molecule at the apical  
98 position completing the square pyramidal coordination geometry ( $\tau = 0$ ) [25]. The Cu-Ocarbox bond  
99 distances range from 1.9546(17) to 1.9774(18), and the angles O-Cu-O(eq) between 88.45 and 90.72°,  
100 while the Cu-OMeOH bond length is larger than previous with a value of 2.1388(17) Å. The metal  
101 atoms are displaced in the axial direction towards the methanol molecules from the oxygen plane, as  
102 indicated by the Ocarbox-Cu-OMeOH angles, with values in the range from 90.07(7) to 100.29(7)°. The  
103 intramolecular Cu $\cdots$ Cu distance is 2.5930(6) Å, which is very similar to values previously reported in  
104 the literature (2.58–2.76 Å) [26–28]. Selected distances and angles are provided in Table 1.

105 The most important intermolecular interaction present in the compound is the hydrogen bond between  
106 methanol's hydroxyl and one of the oxygens from the acetate ligand (O7-H7O $\cdots$ O5, 1.900 Å; O7 $\cdots$ O5,  
107 2.725 Å; O7-H7O-O5, 166.95°). The propagation of these hydrogen bonds defines a two-dimensional  
108 supramolecular network, parallel to the bc plane (Fig. 3, up). The strength of this interaction involves  
109 the approximation of adjacent atoms, and, hence, the formation of O-H7 $\cdots$ C9 and O-H7 $\cdots$ C10  
110 interactions. Furthermore, in these layers weaker CH $\cdots$ O (O1 $\cdots$ H10B 2.515 Å; O6 $\cdots$ H10A, 2.555 Å)  
111 interactions can also be found. The dioxole groups protrude perpendicularly to the layer plane, and  
112 alternatively in opposite directions (Fig. 3, down). The layers are stacked in such a manner that dioxole  
113 groups are interleaved, being able to establish C-H $\cdots$ O interactions that connect the 2D layers yielding a  
114 3D supramolecular network. Hydrogen atoms of the CH<sub>2</sub> coming from the dioxole group (H6A) interact  
115 with acetate's oxygen (O6 $\cdots$ H6A, 2.506 Å). The same hydrogen atom establishes a weak interaction  
116 with carboxylate oxygen from piperonylate group (O2 $\cdots$ H6A, 2.655 Å).

117 Supramolecular networks, with tunable self-organized units, have attracted much attention during the  
118 past years [29–31]. This interest comes from the possibility of fabricate materials with desirable  
119 properties, just by controlling the intermolecular interactions between molecular building units.  
120 Therefore, researchers are focusing on designing new functional complexes with well-defined structures  
121 to accomplish a desired function. In particular, hydrogen bonds play an important role in the formation  
122 of crystal structures [32–34]. The extended 2D supramolecular network of  $[\text{Cu}(\mu\text{-Pip})(\mu\text{-}$   
123  $\text{MeCO}_2)(\text{MeOH})]_2$  shows a great number of H-bond interactions. This strong network explains its  
124 insolubility in methanol and in other tested solvents such as H<sub>2</sub>O, EtOH and DMF. Consequently,

125 during the substitution of acetate ligands for piperonylate ligands, the formation of that strong networks  
126 of H-bond causes the precipitation of the compound. This fact may prevent the formation of the  
127 homoleptic compound, resulting in an easy isolation of this new mixed carboxylate structure. The mixed  
128 carboxylate  $[\text{Cu}(\mu\text{-PhCO}_2)(\mu\text{-MeCO}_2)(\text{CH}_3\text{OH})]_2$  shows a similar 2D supramolecular hydrogen bond  
129 network [10]. Methanol also plays a key role in the hydrogen bonding supramolecular 2D network of  
130  $[\text{Cu}(\mu\text{-C}_8\text{H}_7\text{O}_4)(\mu\text{-MeCO}_2)(\text{CH}_3\text{OH})]_2$  ( $\text{C}_8\text{H}_7\text{O}_4 = \text{vanillic acid}$ ), in this case interacting with the  
131 phenol groups [9].

132 In Fig. 4, the thermal variation of the  $\chi_p T$  is presented for the  $[\text{Cu}(\mu\text{-Pip})(\mu\text{-MeCO}_2)(\text{MeOH})]_2$   
133 compound. The bridging carboxylate groups are very efficient in transmitting super-exchange  
134 interactions between paramagnetic centers [31,35,36]. The magnetic susceptibility of this compound  
135 shows a rounded maximum near room temperature which decreases by lowering the temperature,  
136 reaching a minimum at ca. 50 K and a divergence at lower temperatures. This behavior suggests the  
137 presence of a strong antiferromagnetic  $\text{Cu}\cdots\text{Cu}$  interaction, as expected from the structure of this  
138 compound. The divergence at low temperature indicates the presence of a paramagnetic contribution  
139 from a small percentage of impurities ( $\rho$ ). The magnetic behavior of the compound can be modeled by  
140 the classical Bleaney and Bowers  $S = \frac{1}{2}$  dimer model [37]. In order to reproduce the divergence at low  
141 temperature, we have included a paramagnetic contribution ( $\rho$ ) with the same  $g$  value as the  $\text{Cu(II)}$  ions  
142 in the dimer. The model reproduces very satisfactorily the magnetic properties, in the whole temperature  
143 range, including the divergence at low temperatures with the parameters ( $g=2.12$ ;  $J(\text{cm}^{-1})=-308$ ;  
144  $\rho(\%)=1.13$ ;  $H=-JSiSi+1$ ). These values also agree with the reported values for many other similar  $\text{Cu(II)}$   
145 paddle-wheel dimers, including the original acetate complex ( $J = -284 \text{ cm}^{-1}$ ) [38].

146

147 .

148 **2. CONCLUSIONS**

149

150 In summary, a binuclear complex based in the piperonylate and acetate ligands, with formula [Cu( $\mu$ -  
151 Pip)( $\mu$ -MeCO<sub>2</sub>)(MeOH)]<sub>2</sub>, was prepared and characterized. The compound reported here constitute one  
152 of the very rare examples of mixed carboxylate paddle-wheel copper dimers (8/1300). The dimeric  
153 complex shows a strong intradimer antiferromagnetic Cu...Cu interaction, in agreement with previous  
154 observation in similar dimeric complexes.

155

156 **ACKNOWLEDGEMENTS**

157

158 This work was partially financed by the Spanish National Plan of Research CTQ2014-56324 and Severo  
159 Ochoa SEV-2015-0496, and by the 2014SGR260 and 2014SGR377 projects from the Generalitat de  
160 Catalunya.

161

162 **REFERENCES**

163

- 164 [1] N.R. de Campos, M.A. Ribeiro, W.X.C. Oliveira, D.O. Reis, H.O. Stumpf, A.C. Dorigueto, F.C.  
165 Machado, C.B. Pinheiro, F. Lloret, M. Julve, et al., *Dalton Trans.* 45 (2016) 1782–1789.
- 166 [2] S.S.P. Dias, M.V. Kirillova, V. Andre, J. Klak, A.M. Kirillov, *Inorg. Chem. Frontiers* 2 (2015)  
167 525–537.
- 168 [3] B. Gil-Hernandez, S. Savvin, G. Makhouloufi, P. Nuñez, C. Janiak, J. Sanchiz, *Inorg. Chem.* 54  
169 (2015) 1597–1605.
- 170 [4] R. Bikas, P. Aleshkevych, H. Hosseini-Monfared, J. Sanchiz, R. Szymczak, T. Lis, *Dalton*  
171 *Trans.* 44 (2015) 1782–1789.
- 172 [5] G.-L. Zhuang, W.-X. Chen, J. Zheng, W.-L. Chen, J.-G. Wang, *Inorg. Chem. Commun.* 22  
173 (2012) 18–21.
- 174 [6] K. Hassanein, O. Castillo, C.J. Gómez, F. Zamora, P. Amo-Ochoa, *Cryst. Growth Des.* 15  
175 (2015) 5485–5494.
- 176 [7] Cambridge Structural Database (CSD) (Version 5.36, May 2015).
- 177 [8] I. Galkina, A. Tufatullin, D. Bakhtiyarova, D. Stakheev, V. Galkin, R. Cherkasov, B. Buchner,  
178 O. Kataeva, *CrystEngComm* 16 (2014) 9010–9024.
- 179 [9] B. Kozlevcar, D. Odlazek, A. Golobic, A. Pevec, P. Strauch, P. Segedin, *Polyhedron* 25 (2006)  
180 1161–1166.
- 181 [10] D. Wang, S.-X. Liu, *Chin. J. Struct. Chem.* 25 (2006) 1461–1464.
- 182 [11] G. Vives, S.A. Mason, P.D. Prince, P.C. Junk, J.W. Steed, *Cryst. Growth Des.* 3 (2003) 699–  
183 704.
- 184 [12] D. MasPOCH, D. Ruiz-Molina, K. WurSt, C. Rovira, J. Veciana, *Chem. Commun.* (2002) 2958–  
185 2959.
- 186 [13] D. MasPOCH, D. Ruiz-Molina, K. WurSt, J. Vidal-Molina, C. Rovira, J. Veciana, *Dalton Trans.*  
187 (2004) 1073–1082.
- 188 [14] L.S. Erre, G. Micera, P. Piu, F. Cariati, G. Ciani, *Inorg. Chem.* 24 (1985) 2297–2300.
- 189 [15] A.A. Ageshina, M.A. Uvarova, S.E. Nefedov, *Russ. J. Inorg. Chem.* 60 (2015) 1192–1199.
- 190 [16] J. Soldevila-Sanmartín, J.A. Ayllón, T. Calvet, M. Font-Bardía, J. Pons, Submitted.
- 191 [17] HPip (506 mg, 3.05 mmol) was added to a green solution of Cu(MeCO<sub>2</sub>)<sub>2</sub>·H<sub>2</sub>O (601 mg, 3.01  
192 mmol) in MeOH (60 ml) and stirred for one hour. A green solid appeared that was filtered,  
193 washed with cold methanol and dried at room temperature. Yield: 0.704 (73.5%). This  
194 compound has also been obtained working with other metal to ligand ratios. From mother  
195 liquors, green crystals suitable for single crystal diffraction were obtained. Analysis for  
196 C<sub>22</sub>H<sub>24</sub>O<sub>14</sub>Cu<sub>2</sub> calc/found (%): C, 41.32/41.29; H, 3.78/3.83. ATR-FTIR (cm<sup>-1</sup>): 3279(m),



- 197 1591(s), 1492(w), 1441(m), 1389(s), 1264(m), 1118(m), 1021(s), 922(m), 884(w), 803(w),  
198 775(s), 683(s). Bulk powder XRD pattern is similar to single crystal XRD pattern (Fig. 2).
- 199 [18] K. Nakamoto, *Infrared and Raman Spectra of Inorganic and Coordination Compounds.*  
200 *Applications in Coordination, Organometallic, and Bioinorganic Chemistry*, sixth ed. Wiley-  
201 Interscience, New York, USA, 2009.
- 202 [19] G.B. Deacon, R.J. Phillips, *Coord. Chem. Rev.* 88 (1980) 227–250.
- 203 [20] M. Wriedt, A.A. Yakovenko, G.J. Halder, A.V. Prosvirin, K.R. Dunvar, H.-C. Zhou, *J. Am.*  
204 *Chem. Soc.* 135 (2013) 4040–4050.
- 205 [21] U. Kumar, J. Thomas, N. Thirupathi, *Inorg. Chem.* 49 (2010) 62–72.
- 206 [22] A.R. Katritzky, C.W. Rens, *Comprehensive Heterocyclic Chemistry: The Structure,*  
207 *Reactions, Synthesis, Uses of Heterocyclic Compounds*, Pergamon Press, Oxford, UK, 1984.
- 208 [23] J.A. Pérez, V. Montoya, J.A. Ayllón, M. Font-Bardía, T. Calvet, J. Pons, *Inorg. Chim. Acta* 394  
209 (2013) 21–30.
- 210 [24] Experimental X-ray structure determination of the [Cu( $\mu$ -Pip)( $\mu$ -MeCO<sub>2</sub>)(MeOH)]<sub>2</sub> complex: A  
211 green prism-like crystal (0.103 × 0.104 × 0.126 mm) was measured on a D8 Venture system  
212 equipped with a Multilayer monochromator and a Mo microfocus ( $\lambda = 0.71073 \text{ \AA}$ ).  
213 C<sub>22</sub>H<sub>24</sub>Cu<sub>2</sub>O<sub>14</sub>, M = 639.49, Monoclinic space group P(21/c) with Z = 2, and a = 11.9625(6),  
214 b = 13.0173(7), c = 7.9398(4) Å,  $\beta = 95.112(2)^\circ$ , and V = 1231.46(11) Å<sup>3</sup>. The integration of the  
215 data using a monoclinic unit cell yielded a total of 14640 reflections to a maximum  $\theta$  angle of  
216 26.39° (0.80 Å resolution), of which 2502 were independent (average redundancy 5851,  
217 completeness = 99.6%, R<sub>int</sub> = 4.72%, R<sub>sig</sub> = 3.14%) and 2114 reflections (84.49%) were greater  
218 than 2 $\sigma$ (F<sub>2</sub>). The refinement of the XYZ-centroids of reflections above 20  $\sigma$ (I). Data were  
219 corrected for absorption effects using the multi-scan method (SADABS). The calculated  
220 minimum and maximum transmission coefficients (based on crystal size) are 0.6892 and 0.7454.  
221 The structure was solved using the Bruker SHELXTL, and refined using SHELXL program.  
222 The final anisotropic full-matrix least squares refinement on F<sub>2</sub> with 174 variables converged at  
223 R<sub>1</sub> = 3.05%, for the observed data and wR<sub>2</sub> = 7.34% for all data. The goodness-of-fit was 1.031.  
224 The largest peak in the final difference electron density synthesis was 0.649 eÅ<sup>-3</sup> and the  
225 largest hole was -0.358 eÅ<sup>-3</sup> with a RMS deviation of 0.091 eÅ<sup>-3</sup>. On the basis of the final  
226 model, the calculated density was 1.725 g cm<sup>-3</sup> and F(000) was 652.
- 227 [25] A.W. Addison, T.N. Rao, *J. Chem. Soc. Dalton Trans.* (1984) 1349–1356.
- 228 [26] G. Psomas, C.P. Raptopoulou, C.P. Iordanidis, C. Dendrinou-Samara, V. Tangoulis, D.P.  
229 Kessissoglou, *Inorg. Chem.* 39 (2000) 3042–3048.
- 230 [27] A. Pichon, C.M. Fierro, M. Nieuwenhuyzen, L.J. Stuart, *CrystEngComm* 9 (2007) 449–451.
- 231 [28] S. Gomathi, P.T. Muthiah, *Acta Crystallogr. C* 69 (2011) 1498–1502.
- 232 [29] L. Chen, Q. Chen, M. Wu, F. Jiang, M. Hong, *Acc. Chem. Res.* 48 (2015) 201–210.
- 233 [30] R. Chakrabarty, P.S. Mukherjee, P.J. Stang, *Chem. Rev.* 111 (2011) 6810–6918.
- 234 [31] S. Perez-Yañez, G. Beobide, O. Castillo, J. Cepeda, A. Luque, R. Pascual, *Cryst. Growth Des.*  
235 12 (2012) 3324–3334.

- 236 [32] A.C. Cunha, V.F. Ferreira, A.K. Jordão, M.C.B.V. de Souza, S.M.S.V. Wardell, J.L. Wardell,  
237 P.A. Tan, R.P.A. Bettens, S.K. Seth, E.R.T. Tiekink, *CrystEngComm* 15 (2013) 4917–4929.
- 238 [33] D. Sathukhan, M. Maiti, G. Pilet, A. Bauzá, A. Frontera, S. Mitra, *Eur. J. Inorg. Chem.* 11 (2015)  
239 1958–1972.
- 240 [34] N.M.H. Salem, A.R. Rashad, L. El Sayed, S. Foro, W. Haase, M.F. Iskander, *Inorg. Chim. Acta*  
241 432 (2015) 231–242.
- 242 [35] A. Rodriguez-Forteza, P. Alemany, S. Alvarez, E. Ruiz, *Chem. Eur. J.* 7 (2001) 627.
- 243 [36] H. Li, H. Yao, E. Zhang, Y. Jia, H. Hou, Y. Fan, *Dalton Trans.* 40 (2011) 9388–9393.
- 244 [37] B. Bleaney, K.D. Bowers, *Proc. R. Soc. London, Ser. A.* 214 (1952) 451–465.
- 245 [38] M. Melnik, *Coord. Chem. Rev.* 42 (1982) 259–293
- 246 .

247 **Legends to figures**

248

249 **Figure 1.** ORTEP drawing of  $[\text{Cu}(\mu\text{-Pip})(\mu\text{-MeCO}_2)(\text{MeOH})]_2$ , showing all non-hydrogen atoms and  
250 the atom numbering scheme; 50% probability amplitude displacement ellipsoids are shown.

251

252 **Figure 2.** Comparison of the powder XRD pattern of bulk  $[\text{Cu}(\mu\text{-Pip})(\mu\text{-MeCO}_2)(\text{MeOH})]_2$  (down,  
253 black line) and the pattern simulated from de crystal structure refinement (up, red line). Small  
254 displacement of the peaks was due to the different temperature characterization of the powder (room  
255 temperature) and the monocrystal (100 K).

256

257 **Figure 3.** Supramolecular 2D network generated by the propagation of the hydrogen bond (green line)  
258 between the hydrogen from the methanol ( $\text{O}\cdots\text{H}7$ ) and an oxygen atom of the acetate ligand (O5). Only  
259 the hydrogen atoms involved in this intermolecular interaction are displayed for clarity. Up, projection  
260 down the a axis; down, projections down the b axis, left and the c axis, right.

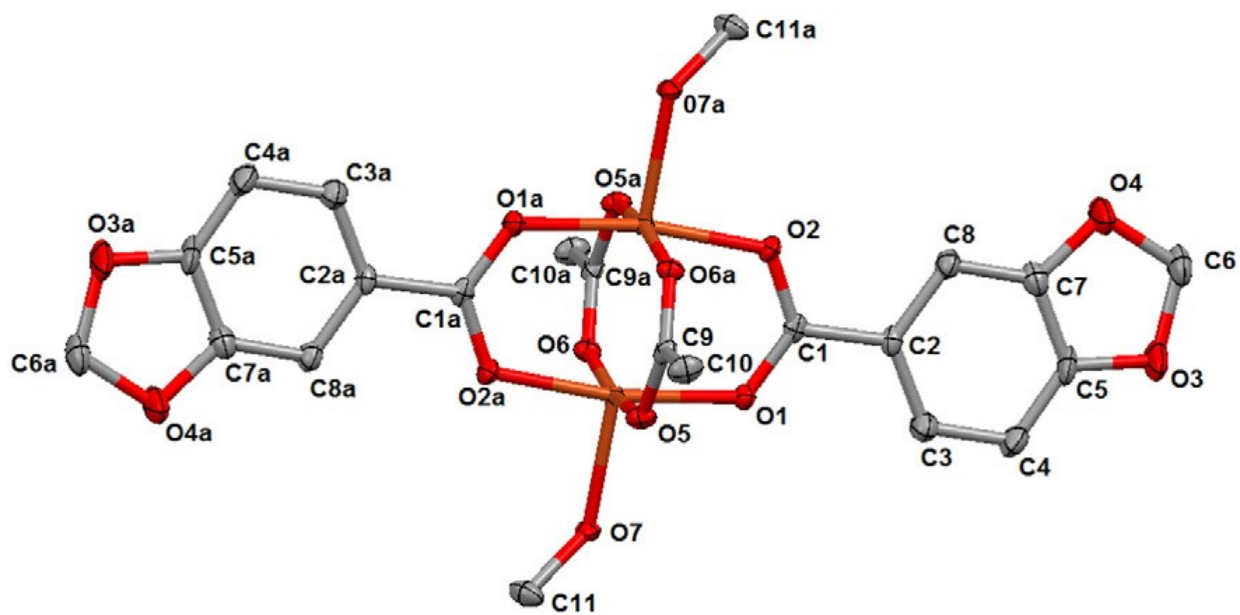
261

262 **Figure 4.** Thermal variation of  $\chi_m T$  for complex  $[\text{Cu}(\mu\text{-Pip})(\mu\text{-MeCO}_2)(\text{MeOH})]_2$ . Solid red line  
263 is the best fit to the  $S = 1/2$  dimer model (see text).

264

265  
266  
267

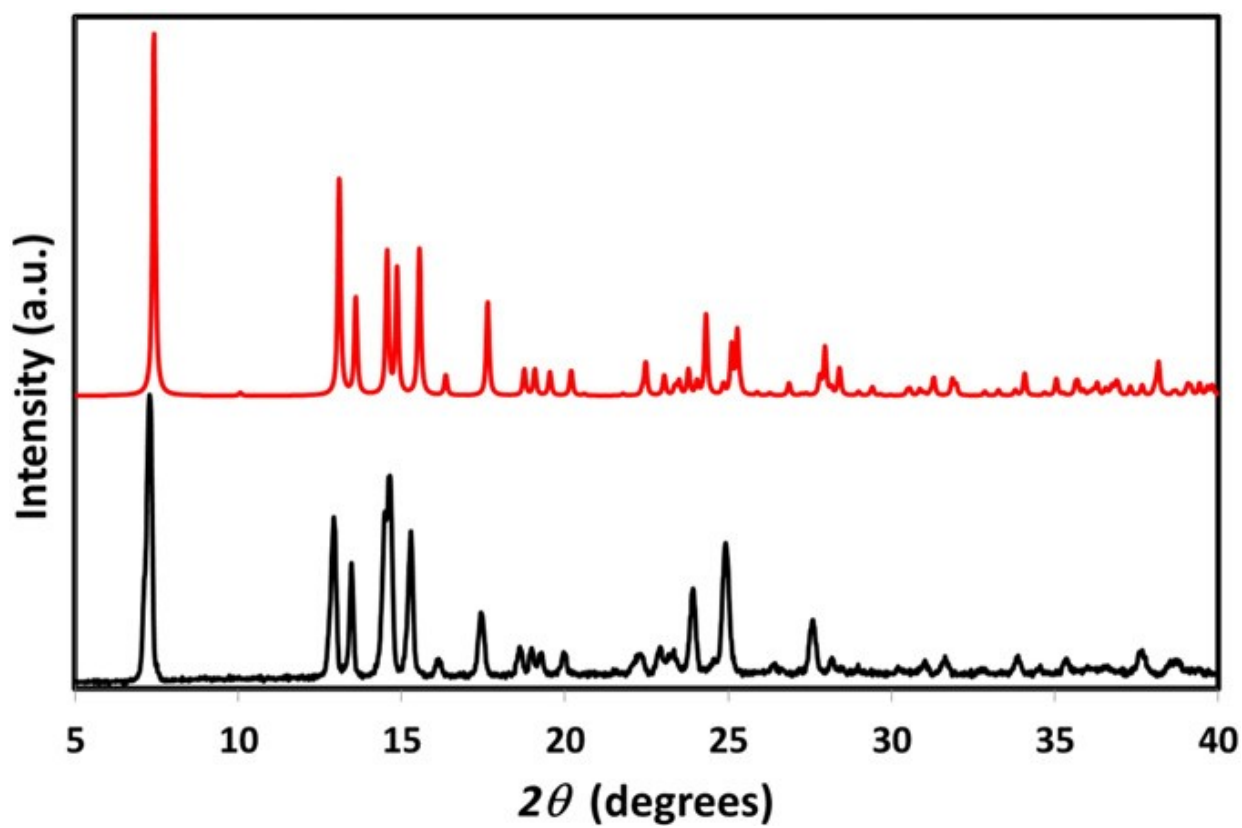
FIGURE 1.



268  
269

270  
271  
272

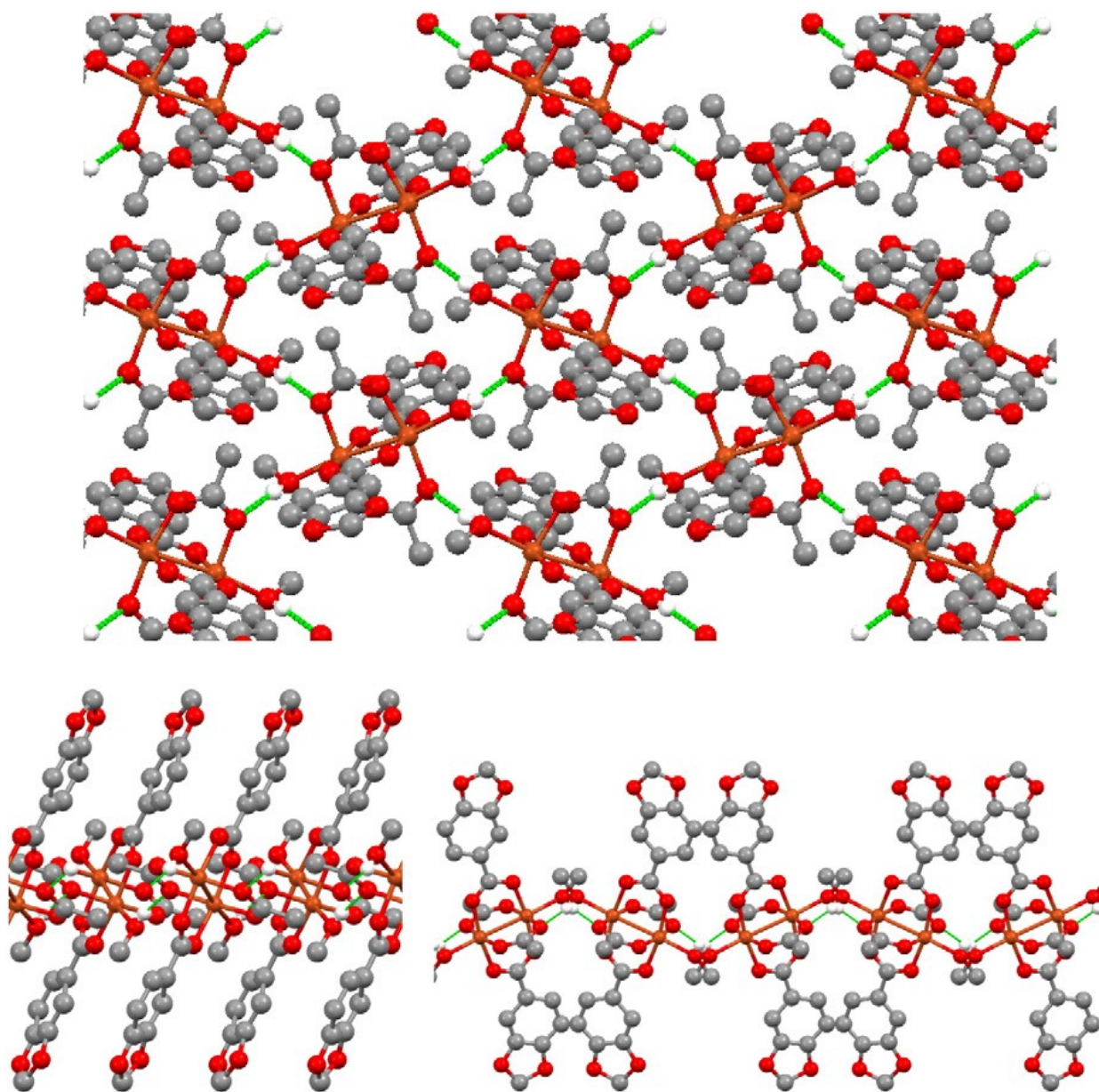
FIGURE 2.



273  
274  
275

276  
277  
278

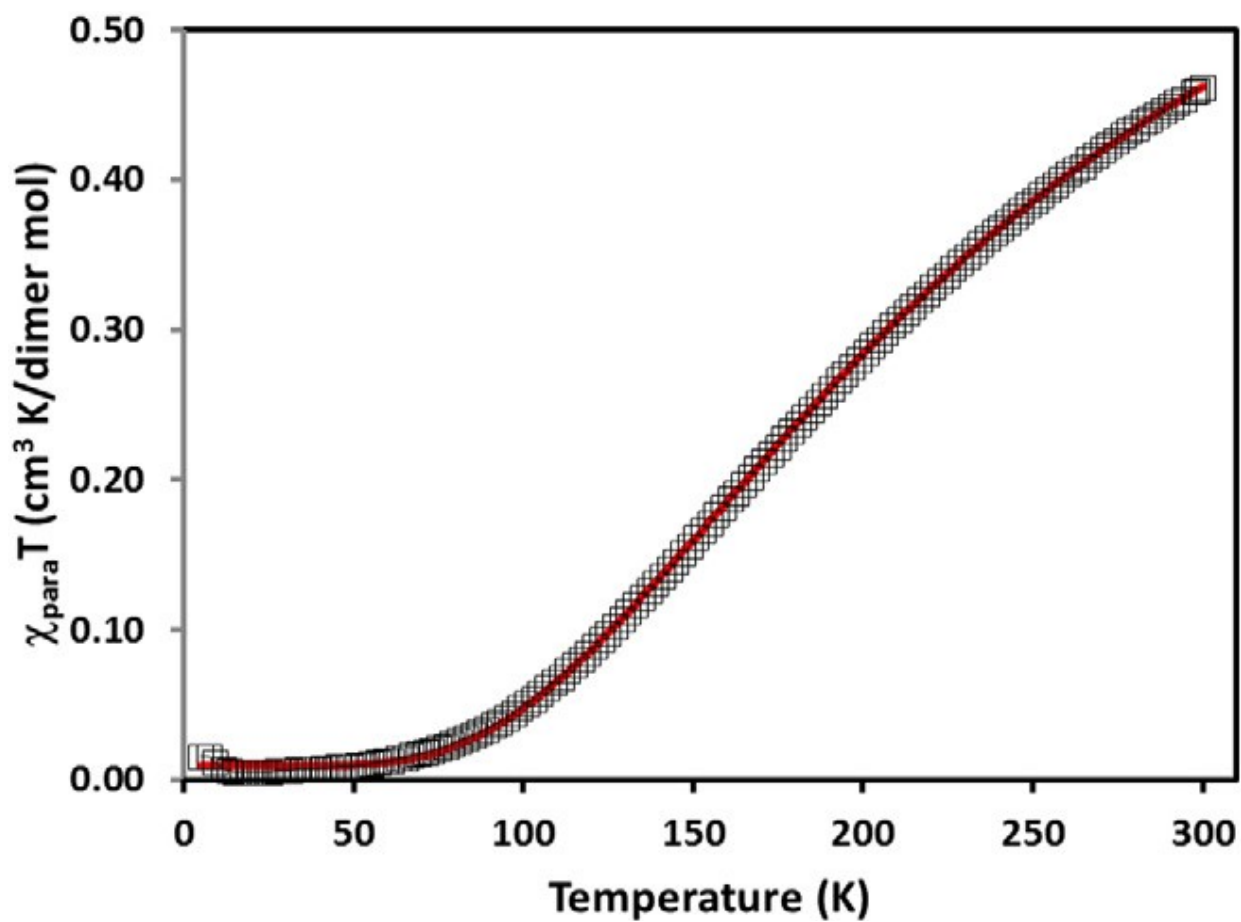
FIGURE 3.



279  
280

281  
282  
283

FIGURE 4.



284  
285

286 **Table 1** Selected bond lengths (Å) and bond angles (°) values for the [Cu(μ-Pip)(μ-MeCO<sub>2</sub>)(MeOH)]<sub>2</sub>  
287 complex. The estimated standard deviations (e.s.d.s.) are shown in parentheses.

288

Bond lengths (Å)			
Cu(1)-O(2)	1.9546(17)	Cu(1)-O(5)	1.9774(18)
Cu(1)-O(1)#1	1.9603(18)	Cu(1)-O(7)	2.1388(17)
Cu(1)-O(6)#1	1.9720(18)	Cu(1)-Cu(1)#1	2.5930(6)
Bond angles (°)			
O(2)-Cu(1)-O(1)#1	169.55(7)	O(6)#1-Cu(1)-O(5)	169.55(7)
O(2)-Cu(1)-O(6)#1	89.45(8)	O(2)-Cu(1)-O(7)	94.48(7)
O(1)#1-Cu(1)-O(6)#1	90.72(7)	O(1)#1-Cu(1)-O(7)	95.96(7)
O(2)-Cu(1)-O(5)	88.45(8)	O(6)#1-Cu(1)-O(7)	90.07(7)
O(1)#1-Cu(1)-O(5)	89.50(8)	O(5)-Cu(1)-O(7)	100.29(7)

289

290

291

292

293

294